



**You have downloaded a document from
RE-BUŚ
repository of the University of Silesia in Katowice**

Title: Polarization effects in $e+e\text{-to } W+W\text{\$}$

Author: Karol Kołodziej

Citation style: Kołodziej Karol. (1994). Polarization effects in $e+e\text{-to } W+W\text{\$}$. "Acta Physica Polonica. B" (1994, no. 9, s. 1345-1359).



Uznanie autorstwa - Licencja ta pozwala na kopiowanie, zmienianie, rozprowadzanie, przedstawianie i wykonywanie utworu jedynie pod warunkiem oznaczenia autorstwa.



UNIwersYTET ŚLĄSKI
W KATOWICACH



Biblioteka
Uniwersytetu Śląskiego



Ministerstwo Nauki
i Szkolnictwa Wyższego

POLARIZATION EFFECTS IN $e^+e^- \rightarrow W^+W^-^{*,**,\dagger}$

K. KOŁODZIEJ@

Sektion Physik der Universität München
Theresienstr. 37, D-80333 München, Germany

(Received June 15, 1994)

We investigate longitudinal and transverse beam polarization in $e^+e^- \rightarrow W^+W^-$ including electroweak radiative corrections and hard bremsstrahlung. Also final state polarizations are discussed. We show that the transverse beam polarization allows to study the most interesting longitudinal-longitudinal final state polarization without looking at the polarization of the final state particles. However, to detect possible small deviations from the standard model a high luminosity e^+e^- -collider, with energy scan from the peak of the cross-section up to about 300 GeV, is necessary.

PACS numbers: 12.15. Ji

1. Introduction

The main process to be measured at LEP 200 is $e^+e^- \rightarrow W^+W^-$ (see Fig. 1). It should provide the first direct experimental test of the triple gauge coupling of the $SU(2)_L \times U(1)_Y$ non-abelian gauge group of the electroweak standard model (SM) [1]. Up to now this coupling has been tested only indirectly, through loop effects, at LEP 100. The loop effects induced by possible deviations from the Yang-Mills structure are not easy to distinguish from other possible non standard effects. However, since the precision measurements at the Z -threshold agree excellently with theory,

* Presented at the XVII International School of Theoretical Physics "Standard Model & Beyond '93", Szczyrk, Poland, 19-27 September, 1993.

** Based on work in collaboration with J. Fleischer, F. Jegerlehner and M. Zralek.

† Work supported by the German Federal Ministry for Research and Technology under contract No. 05 6MU 93P.

@ On leave from the Institute of Physics, University of Silesia, ul. Uniwersytecka 4, PL-40007 Katowice, Poland.

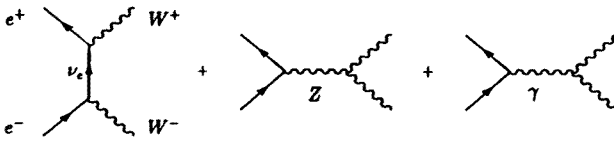


Fig. 1. The lowest order Feynman diagrams for the process $e^+e^- \rightarrow W^+W^-$.

there is no much room left for deviations from the SM when going to LEP 200 [2].

In the limit of vanishing electron mass, $m_e = 0$, where there is no Higgs' contribution to the lowest order cross section, given the experimentally well established $W e \nu$ -coupling of the t -channel diagram, renormalizability uniquely fixes the triple gauge couplings $W^+W^-\gamma$ and W^+W^-Z present in the s -channel diagrams. However, in order to perform a model independent analysis, at least at tree level, the triple gauge couplings should be parametrized in a most general way [23]. Any deviations from renormalizability, *e.g.* from the Yang-Mills form of the couplings, would usually result in dramatic increase of the cross section at high energies, which would violate unitarity [3]. This effect can be diminished if different 'anomalous' couplings conspire with each other. The cross section may increase also due to other effects, *e.g.* presence of the extra heavy fermion family without large mass splitting within a doublet, which is excluded by limits on the ρ parameter. In this case the unitarity is restored only at energies above the heavy particle threshold [4].

In order to disentangle the triple gauge couplings one has to face the following problems. First of all, the notion of form factors is meaningful only in the 'classical' limit *e.g.* at zero momentum transfer or at the Z pole, where the experiment can be set up in such a way that mainly the effect of a single particle exchange is detected. For $e^+e^- \rightarrow W^+W^-$ we are far above the Z threshold, electroweak unification is at work and γ and Z contributions conspire, which make it very difficult to separate them. Secondly, investigation of the most interesting $e^+e^- \rightarrow W_L^+W_L^-$ and $e^+e_R^- \rightarrow W^+W^-$ modes in LEP 200 will be limited because of very low statistics. Moreover, the s -channel contributions which contain the triple gauge couplings are suppressed at the W -pair threshold and grow fast with energy. Therefore to study them it is desirable to go to as high energies as possible. Since transverse polarization is natural polarization in e^+e^- storage rings, where electrons and positrons tend to align in opposite directions with an external magnetic field, it can provide an extra tool for studying the triple gauge boson couplings. To achieve a 1% sensitivity to deviations from the SM one needs high precision experiments which might require higher luminosities as well as theoretical predictions at the same or even better level of accuracy.

The latter implies that the radiative corrections has to be included in the analysis of future data [5].

Since W -bosons are unstable particles, observed is actually the process $e^+e^- \rightarrow 4f(\gamma)$. Sufficiently above the threshold, $e^+e^- \rightarrow W^+W^- \rightarrow 4f(\gamma)$ with both W 's at resonance dominates and for the sake of the following discussion we assume both W 's to be on mass shell particles. However, we realize that this assumption is valid only at the level of a few per cent and in the actual analysis of the data also the decays of W -bosons have to be taken into account [6, 7].

In Sec. 2 of this talk we discuss polarized W -pair production cross sections together with virtual radiative corrections. In Sec. 3 transverse and longitudinal asymmetries are defined. Bremsstrahlung and mass effects are included in Sec. 4. Finally, in Sec. 5 we present SM results for various polarized cross sections and asymmetries.

2. Polarized W -pair production cross sections and $O(\alpha)$ radiative corrections

SM electroweak virtual corrections to the process

$$e^+(p_+, \bar{\sigma}) + e^-(p_-, \bar{\sigma}) \rightarrow W^+(q_+, \bar{\lambda}) + W^-(q_-, \lambda), \quad (1)$$

where in parenthesis we indicated particles momenta and helicities, have been calculated in [8–10]. The results of the two last papers agree in general up to 10^{-4} . The largest discrepancy of 0.3% appears at 500 GeV and 179° , where the cross section is small anyway and one does not expect statistics to be high enough for experimental accuracy to match this level of precision.

The polarized differential cross section for producing the W^- -boson at angle θ with respect to the electron and velocity $\beta_W = \sqrt{1 - 4M_W^2/s}$, $s = (p_- + p_+)^2$, in the e^+e^- centre of mass system (CMS) is given by

$$\frac{d\sigma(h_e; \lambda, \bar{\lambda})}{d(\cos \theta)} = \frac{\beta_W}{32\pi s} \left| \sum_{i=1}^6 X_i^{(h_e)} M_i(h_e; \lambda, \bar{\lambda}) \right|^2, \quad (2)$$

where $X_i^{(h_e)} = S_1^{(h_e)}, \dots, S_4^{(h_e)}, T_1^{(h_e)}, X_6^{(h_e)}$ and $M_i(h_e; \lambda, \bar{\lambda})$, $i = 1, 2, \dots, 6$, $h_e = 2\sigma = \pm 1$, are Lorentz invariant and helicity amplitudes, respectively. In the limit $m_e = 0$, the nonvanishing helicity matrix elements are obtained only for opposite electron and positron helicities, $\bar{\sigma} = -\sigma$,

$$M_i(h_e; \lambda, \bar{\lambda}) = \bar{v}(p_+, -\sigma) O_i^{\mu\nu} P_{h_e} u(p_-, \sigma) \varepsilon_\mu^*(q_+, \bar{\lambda}) \varepsilon_\nu^*(q_-, \lambda). \quad (3)$$

In Eq. (3) $P_{h_e} = \frac{1}{2}(1 + h_e \gamma_5)$ are chiral projectors and $O_i^{\mu\nu}$, $i = 1, 2, \dots, 6$, are 4×4 -matrix valued second rank tensors given by

$$\begin{aligned} O_1^{\mu\nu} &= [r^\alpha g^{\mu\nu} + 2(g^{\mu\alpha} P^\nu - g^{\nu\alpha} P^\mu)] \gamma_\alpha \equiv O_1^{\mu\nu\alpha} \gamma_\alpha, \\ O_2^{\mu\nu} &= (g^{\mu\alpha} P^\nu - g^{\nu\alpha} P^\mu) \gamma_\alpha \equiv O_2^{\mu\nu\alpha} \gamma_\alpha, \\ O_3^{\mu\nu} &= \frac{P^\mu P^\nu}{P^2} r^\alpha \gamma_\alpha \equiv O_3^{\mu\nu\alpha} \gamma_\alpha, \\ O_4^{\mu\nu} &= i \varepsilon^{\mu\nu\alpha\beta} r_\beta \gamma_\alpha \equiv O_4^{\mu\nu\alpha} \gamma_\alpha, \quad \varepsilon_{0123} = 1, \\ O_5^{\mu\nu} &= \gamma^\mu (\not{p}_- - \not{q}_-) \gamma^\nu, \\ O_6^{\mu\nu} &= \not{r} \frac{Q^\mu Q^\nu}{P^2}, \end{aligned} \quad (4)$$

where we have used the combinations of particle momenta: $P = p_+ + p_-$, $Q = p_+ - p_-$ and $r = q_- - q_+$. We have eliminated the other two tensors which were originally used in [10], so that the tensors listed in Eq. (4) make up a complete base for representing the SM one-loop corrections to $e^+ e^- \rightarrow W^+ W^-$.

In the Born approximation, which obviously determines main features of the process under consideration, only the amplitudes $S_1^{(\pm)}$ and $T_1^{(-)}$ are non zero. In the high energy limit, $s \rightarrow \infty$ ($\beta_W \rightarrow 1$, $\gamma_W \rightarrow \infty$), they have the following form

$$\begin{aligned} S_{1(0)}^{(+)} &= -\frac{e^2}{s} \left(1 - \frac{1}{1 - \frac{M_Z^2}{s}} \right) \rightarrow 0, \\ S_{1(0)}^{(-)} &= S_{1(0)}^{(+)} - \frac{g^2}{2s} \frac{1}{1 - \frac{M_Z^2}{s}} \rightarrow -\frac{g^2}{2s}, \\ T_{1(0)}^{(-)} &= \frac{g^2}{s} \frac{1}{\frac{1+\beta_W^2}{2} - \beta_W \cos \theta} \rightarrow \frac{g^2}{s} \frac{1}{1 - \cos \theta}, \end{aligned} \quad (5)$$

where the limits are understood as a leading behaviour in s . Moreover, for the final polarization states with $|\Delta\lambda| = |\lambda - \bar{\lambda}| < 2$, we find (see Ref. [10])

$$\frac{M_5(h_e; \lambda, \bar{\lambda})}{M_1(h_e; \lambda, \bar{\lambda})} \rightarrow \frac{1 - \cos \theta}{2}, \quad \text{for } \gamma \rightarrow \infty (\beta \rightarrow 1). \quad (6)$$

If we insert the asymptotic forms of Eqs (5) and (6) to the sum on the right hand side of Eq. (2) which, dependent on the initial electron polarization, takes the form

$$S_{1(0)}^{(-)} M_1(-; \lambda, \bar{\lambda}) + T_{1(0)}^{(-)} M_5(-; \lambda, \bar{\lambda}) \quad \text{or} \quad S_{1(0)}^{(+)} M_1(+; \lambda, \bar{\lambda}),$$

we will see how gauge cancellations work already at the level of helicity amplitudes. For $\Delta\lambda = \pm 2$ the s -channel helicity amplitudes vanish and there is no gauge cancellations between the s - and t -channel contributions. This is the main reason why the transverse-transverse (TT), $\lambda = \pm 1$, $\bar{\lambda} = \pm 1$, final state polarization is the dominant contribution to the unpolarized cross section. In the high energy limit only this and the longitudinal-longitudinal (LL), $\lambda = \bar{\lambda} = 0$, mode survive. In the $m_e = 0$ limit, the helicity amplitude of the right-handed initial state polarization ($h_e = +1$) does not contain the dominant t -channel contribution since the $e\nu W$ -coupling contains only the left-handed chiral projector and the gauge cancellations take place only between the γ and Z s -channel contributions. Thus, given the $W^+W^-\gamma$ coupling which is fixed by electromagnetic gauge invariance, by measuring the right-handed cross section, we could fix the unknown W^+W^-Z coupling. However, the mode $e^+e^-_R \rightarrow W^+W^-$ is suppressed by two orders of magnitude with respect to the unpolarized cross section, which would make it very difficult to measure the cross section for this polarization.

In the one-loop order the s -channel amplitudes $S_1^{(\pm)}, \dots, S_4^{(\pm)}$ receive contributions from γ - and Z -self energies, $e^+e^-\gamma$ -, e^+e^-Z -, $W^+W^-\gamma$ - and W^+W^-Z -vertices as well as from 'boxes'. The t -channel amplitude $T_1^{(-)}$ gets contributions from the neutrino self energy, $e\nu W$ -vertices and 'boxes', whereas $T_1^{(+)}$ and $X_6^{(\pm)}$ are pure 'box' amplitudes. Only the amplitudes $S_1^{(\pm)}$ and $T_1^{(-)}$ which are present at tree level contain ultraviolet and infrared divergences in the one-loop order. Renormalization is performed in the G_μ -scheme [10], where physical particle masses and the Fermi coupling G_μ determined from muon decay are used as input parameters.

The triple gauge boson vertices $W^+W^-\gamma$ and W^+W^-Z at the one-loop level of the SM can be parametrized in the following way [11]:

$$i\Gamma_V^{\mu\nu\alpha} = ic_V[A_1^V O_1^{\mu\nu\alpha} + A_2^V O_2^{\mu\nu\alpha} + A_3^V O_3^{\mu\nu\alpha} + A_4^V O_4^{\mu\nu\alpha}], \quad (7)$$

where $V = \gamma, Z$, $c_\gamma = e$ and $c_Z = e(\cos\theta_W/\sin\theta_W)$, θ_W being the weak mixing angle. Because of the box contributions, form factors A_i^V depend both on s and $t = (p_- - q_-)^2$. The one-loop induced SM vertices of Eq. (7) conserve the combined Landau parity CP . If one admitted the CP violation there would be three $W^+W^-\gamma$ and three W^+W^-Z form factors in addition [12]. With parametrization (7) and definitions (4) each s -channel amplitude picks up exactly one form factor. The form factors contribute to helicity amplitudes, squares of which are measurable, in different combinations, dependent on polarization state [17].

$$\begin{aligned}
\sum_{i=1}^6 X_i^{(-)} M_i(-; \lambda, \bar{\lambda}) &= C_{\lambda, \bar{\lambda}}^{h_e}(\theta) \left\{ e^2 \left(H_i^\gamma(\lambda, \bar{\lambda}) - \frac{H_i^Z(\lambda, \bar{\lambda})}{1 - M_Z^2/s} \right) \right. \\
&\quad \left. + \frac{g^2}{2} \frac{H_i^Z(\lambda, \bar{\lambda})}{1 - M_Z^2/s} - \frac{s}{\beta_W} T_1^{(-)} \hat{M}_5(-; \lambda, \bar{\lambda}) \right\} + \dots \\
\sum_{i=1}^6 X_i^{(+)} M_i(+; \lambda, \bar{\lambda}) &= C_{\lambda, \bar{\lambda}}^{h_e}(\theta) e^2 \left(H_i^\gamma(\lambda, \bar{\lambda}) - \frac{H_i^Z(\lambda, \bar{\lambda})}{1 - M_Z^2/s} \right) + \dots, \quad (8)
\end{aligned}$$

where $C_{\lambda, \bar{\lambda}}^{h_e}(\theta) = \sqrt{2} \beta_W \gamma_W^{2-|\lambda| - |\bar{\lambda}|} d_{h_e, \Delta\lambda}^{J_0}(\theta)$ with $\gamma_W = (1 - \beta_W^2)^{-\frac{1}{2}}$ being the Lorentz factor, $d_{h_e, \Delta\lambda}^{J_0}(\theta)$ a rotation matrix by angle θ around the second axis, $\Delta\lambda = \lambda - \bar{\lambda}$ and $J_0 = \max(|h_e|, |\Delta\lambda|)$; $\hat{M}_5(-; \lambda, \bar{\lambda})$ is a reduced helicity amplitude defined by

$$M_5(-; \lambda, \bar{\lambda}) = C_{\lambda, \bar{\lambda}}^{h_e}(\theta) \hat{M}_5(-; \lambda, \bar{\lambda}) \quad (9)$$

and H_i^V are dependent on final state polarization combinations of the form factors given by

$$\begin{aligned}
H_i^V(0, 0) &= (2 + \gamma_W^{-2}) A_1^V + 2A_2^V - \beta_W^2 A_3^V, \\
H_i^V(\pm, \pm) &= A_1^V, \\
H_i^V(\pm, 0) &= 2A_1^V + A_2^V \mp \beta_W A_4^V, \\
H_i^V(0, \pm) &= 2A_1^V + A_2^V \pm \beta_W A_4^V, \\
H_i^V(\pm, \mp) &= 0. \quad (10)
\end{aligned}$$

As it has been shown in [13] the terms denoted in Eq. (8) by the ellipsis can be safely neglected in the energy region from the threshold up to 1 TeV. We would like to stress once more that the SM form factors A_i^V of W^+W^-V -vertices contain also contributions from other radiatively induced vertices as well as self energies and 'boxes'. The amplitudes H_i^γ and H_i^Z are determined relative to each other and the SM ν -exchange contribution. Notice that near the threshold, where $\beta_W \rightarrow 0$, the terms containing H_i^γ and H_i^Z in Eq. (8) are suppressed by factor β_W . Similarly, the contributions of form factors A_3^V and A_4^V are suppressed by β_W^2 and β_W , respectively. From Eq. (8) we see that the gauge cancellations in the one-loop order work like the ones at the tree level.

In the limit $m_e = 0$ we have $2 \times 3 \times 3 = 18$ polarized cross sections. The CP-invariance which is satisfied in the one-loop order of the SM implies the following relations between the helicity amplitudes

$$M(\sigma, \bar{\sigma}; \lambda, \bar{\lambda}) = M(-\bar{\sigma}, -\sigma; -\bar{\lambda}, -\lambda). \quad (11)$$

Eq. (11) reduces the number of independent helicity amplitudes to 12. This is also the number of independent polarized cross sections. The possible CP even deviations from the SM couplings $W^+W^-\gamma$ or W^+W^-Z add to the loop induced form factors. If the CP violating couplings were present one would observe deviations from the relations implied by Eq. (11)

$$\frac{\sigma(h_e; -, -)}{\sigma(h_e; +, +)} = \frac{\sigma(h_e; -, 0)}{\sigma(h_e; 0, +)} = \frac{\sigma(h_e; 0, -)}{\sigma(h_e; +, 0)} = 1. \quad (12)$$

The 4 TT ($\Delta\lambda = \pm 2$) polarizations do not contain contributions from the interesting s -channel amplitudes. Thus, there remain 8 polarized cross sections, which, in principle should be enough to determine 8 independent form factors A_i^V , $i = 1, \dots, 4$, $V = \gamma, Z$. However, many polarized cross sections are substantially suppressed (see Fig. 4). The best possibility to determine them seems to be a detailed investigation of the $e^+e^- \rightarrow W^+W^-$ peak around 200 GeV up to about 300 GeV with a factor 100 increased luminosity compared to LEP 200. However, if deviations from the SM couplings are present, new high energy e^+e^- -colliders will have a much higher sensitivity to them.

3. Transverse polarization

For natural polarization in e^+e^- storage rings the polarization vectors of the electrons and positrons point in opposite directions due to the different sign of the respective magnetic moments. For the sake of the following discussion we fix our reference frame in the e^+e^- CMS such that the z -axis is aligned with the e^- -momentum, y -axis is antiparallel to the external magnetic field of the storage ring and the x -axis points from the centre of the ring outwards as it is illustrated in Fig. 2.

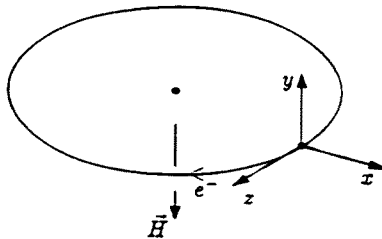


Fig. 2. The reference frame for polarization.

Let us consider first the transition amplitudes for collisions of arbitrarily polarized beams [14]. In the helicity base the electron density matrix is given by

$$\rho_{\sigma\sigma'} = \frac{1 + \vec{\sigma} \cdot \vec{P}}{2} = \frac{1}{2} \begin{pmatrix} 1 + P_L & P_T e^{-i\phi} \\ P_T e^{+i\phi} & 1 - P_L \end{pmatrix} \quad (13)$$

with $\vec{P} = (P_T \cos \phi, P_T \sin \phi, P_L)$, P_L the longitudinal polarization and P_T the magnitude of the transverse polarization. The density matrix for the positron has the same form with corresponding polarization vector $\vec{P}' = (P'_T \cos \phi', -P'_T \sin \phi', P'_L)$ and polarization angle ϕ' . We note that $|\vec{P}| = ((P_T)^2 + (P_L)^2)^{1/2} \leq 1$ and $|\vec{P}| = 1$ for a pure state of complete polarization in a given direction. The square of the matrix element for polarized beams is

$$|\overline{M}|^2 = \sum \rho_{\sigma\sigma'} \bar{\rho}_{\bar{\sigma}\bar{\sigma}'} M_{\sigma\bar{\sigma}} M_{\sigma'\bar{\sigma}'}^*, \quad (14)$$

where $M_{\sigma\bar{\sigma}}$ are the helicity amplitudes, which are independent of ϕ and ϕ' but depend on the azimuthal production angle ϕ_W of the W^- . However, we may perform a rotation around the beam axis $(x, y) \rightarrow (x', y')$ such that the amplitudes can be evaluated at zero azimuthal angle as usual (see Sec. 2). Doing so we have to replace $\phi \rightarrow \phi - \phi_W$ and $\phi' \rightarrow \phi' + \phi_W$. Substituting expressions for the electron and positron density matrices to Eq. (14) and making use of the fact that in the limit $m_e \rightarrow 0$ only the amplitudes $M_- = M_{-+}$ and $M_+ = M_{+-}$ are nonzero, we obtain

$$|\overline{M}|^2 = \frac{1}{4} [(1 - P_L P'_L) (|M_+|^2 + |M_-|^2) + (P_L - P'_L) (|M_+|^2 - |M_-|^2) + (2P_T P'_T) (\cos(\Delta\phi) \operatorname{Re}(M_+ M_-^*) + \sin(\Delta\phi) \operatorname{Im}(M_+ M_-^*))] \quad (15)$$

where $\Delta\phi = \phi - \phi' - 2\phi_W$. The last term proportional to $\operatorname{Im}(M_+ M_-^*)$ is CP-violating.

For natural polarization in a storage ring we have $\vec{P}_T \parallel -\vec{H}$ and $\vec{P}'_T \parallel \vec{H}$ such that $\phi = \phi' = \frac{\pi}{2}$ and hence

$$|\overline{M}|^2 = \frac{1}{4} [(1 - P_L P'_L) (|M_+|^2 + |M_-|^2) + (P_L - P'_L) (|M_+|^2 - |M_-|^2) + (2P_T P'_T) (\cos(2\phi_W) \operatorname{Re}(M_+ M_-^*) - \sin(2\phi_W) \operatorname{Im}(M_+ M_-^*))] \quad (16)$$

Thus with unpolarized beams one measures $|M_-|^2 + |M_+|^2$ via the cross section

$$\frac{d\sigma}{d\cos\theta} = \frac{1}{2} \left(\frac{d\sigma_L}{d\cos\theta} + \frac{d\sigma_R}{d\cos\theta} \right) = \frac{\beta}{64\pi s} (|M_-|^2 + |M_+|^2), \quad (17)$$

with polarized beams one can measure $|M_-|^2 - |M_+|^2$ via the left-right asymmetry A_{LR} defined by

$$\frac{d(\sigma A_{LR})}{d\cos\theta} = \frac{1}{2} \left(\frac{d\sigma_L}{d\cos\theta} - \frac{d\sigma_R}{d\cos\theta} \right) = \frac{\beta}{64\pi s} (|M_-|^2 - |M_+|^2), \quad (18)$$

while $\operatorname{Re}(M_+ M_-^*)$ is measurable with transversely polarized beams from the azimuthal asymmetry A_T defined by

$$\frac{d(\sigma A_T)}{d\cos\theta} = \int_0^{2\pi} \frac{d^2\sigma}{d\cos\theta d\phi_W} \cos 2\phi_W d\phi_W = \frac{\beta}{64\pi s} 2 \operatorname{Re}(M_+ M_-^*). \quad (19)$$

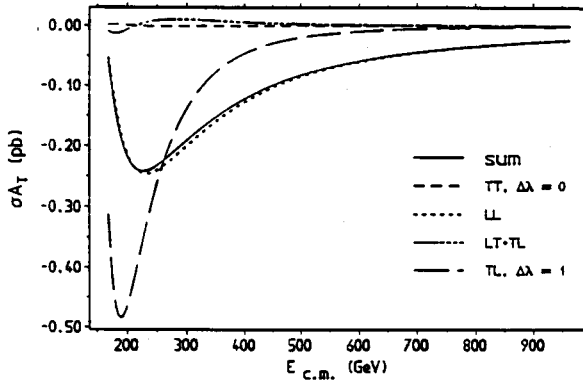


Fig. 3. Contributions from TT, LL and LT + TL final states to transverse asymmetry σA_T at tree level.

A transversely polarized state is a linear combination of the two helicity states and therefore transverse polarization provides an interesting possibility to measure the relative phase of the helicity amplitudes. However, to the extent that the electron is massless, the leptonic chiral symmetry implies that the transversely polarized cross-section averaged over the azimuthal angle is equal to the total unpolarized cross-section. Any deviation from this 'sum rule' is a clear signal for 'new physics' which breaks the leptonic chiral symmetry [15].

Properties of the transverse asymmetry σA_T defined in Eq. (19) can be again understood from its Born approximation [17] (see Fig. 3). The TT final state with $\Delta\lambda = \pm 2$ does not contribute since $M(+; \pm, \mp) = 0$. Contributions of the final states with one longitudinal and one transverse W -boson (LT and TL) cancel each other. In the result the sum over final state polarizations is dominated by the LL polarization. Thus, the transverse asymmetry probes the most interesting LL mode without analyzing the final state polarizations. Unfortunately, $|A_T|$ is rather small, of the order of 1%. At LEP 200 it thus can be measured at best with 10% accuracy. Numerical comparison with σ_R performed in [17] shows that σA_T is slightly disfavoured at LEP energies but wins above 400 GeV.

4. Bremsstrahlung and mass effects

In order to cancel the infrared divergence of the one-loop virtual corrections the soft bremsstrahlung cross section has to be added to the virtual corrected one. In that way also the large Sudakov double logarithms are cancelled. The soft bremsstrahlung correction to differential cross-section (2) has been calculated in an analytic form in [9, 10].

As the hard bremsstrahlung process $e^+e^- \rightarrow W^+W^-\gamma$, where the photon goes into the beam pipe, has energy grater than the soft photon cut E_{cut} , but still below a detection threshold, or cannot be experimentally distinguished from the decay product of the W 's, can imitate the final state of process (1), the corresponding correction has to be taken into account, too. The helicity matrix element of the hard bremsstrahlung process has been calculated using the method developed in [19]. The phase space integration has been done with the use of the Monte Carlo routine VEGAS [20], which allows to incorporate kinematical cuts in an easy way. During the integration care has to be taken in order to diminish an effect of the peaks which arise for the photon collinear to the beam, for the low energy photon and, in the high energy range, for the W^- -boson collinear with the electron beam.

Of course, the sum of soft and hard bremsstrahlung corrections has to be independent on E_{cut} , which has been in detail checked in [18] and [16] where the hard bremsstrahlung correction has been added to the existing calculations of electroweak corrections of [9] and [10], respectively.

Since we are mostly interested in the kinematical situation where the photon is collinear to the beam, we have to take into account the non zero electron mass correction. The latter arises when the scalar product (kp) of the photon and electron or positron momenta, k and p , respectively, appearing in denominator of the matrix element becomes of the order of m_e^2 . Remind that terms containing powers of m_e has been neglected up to now. In case of polarized beams this correction has been studied extensively in [21]. For the photon parallel to the electron or positron, the polarized matrix element squared which accounts for the non zero m_e correction can be expressed in terms of the matrix element of the non radiative process with $m_e = 0$ and appropriate change of the momenta and polarization vectors.

$$\sum |M_{\text{rad}, m_e \neq 0}|^2 = \frac{e^2}{(kp)(1-x)} A \sum |M_{0, m_e=0}|_{p \rightarrow p-k, \vec{P} \rightarrow \vec{P}^{(\text{eff})}}^2, \quad (20)$$

where

$$\begin{aligned} A &= \frac{1 + (1-x)^2}{x} - \frac{m_e^2}{kp}(1-x), \\ P_L^{(\text{eff})} &= \frac{1}{A} \left\{ \frac{1 + (1-x)^2}{x} - \frac{m_e^2}{kp}(1-x+x^2) \right\}, \\ P_T^{(\text{eff})} &= \frac{1}{A} \left\{ \frac{2(1-x)}{x} - \frac{m_e^2}{kp}(1-x) \right\}, \end{aligned} \quad (21)$$

with $x = k^0/E_{\text{beam}}$ being the fraction of beam energy carried by the photon. We have checked numerically that the replacement of the polarization

components by the effective ones changes the result at the CM energy of 200 GeV by at most 0.0004% which is more than 3 orders of magnitude below the expected accuracy of the LEP 200. Thus the change to the effective components of the polarization vector, which depend both on x and $\cos\theta_\gamma$, with θ_γ being the photon angle with respect to the beam, can be safely neglected. This allows to save a computer time during the MC integration since the results of the integration can be combined with different degrees of the beam polarization.

5. Standard model results

As it has been shown in [10] and [16] $O(\alpha)$ corrected results depend very little on the renormalization scheme choice. Therefore in Figs 4–8 we present the results in the G_μ -scheme only. The relevant parameters used are

$$G_\mu = 1.166389 \cdot 10^{-5} \text{ GeV}^{-2},$$

$$M_Z = 91.176 \text{ GeV}, \quad m_H = 100 \text{ GeV}, \quad m_t = 130 \text{ GeV}.$$

This gives $M_W = 80.151 \text{ GeV}$. The values of the remaining fermion masses are the same as in [17]. For the evaluation of the one-loop integrals we have used the package FF by van Oldenborgh [22].

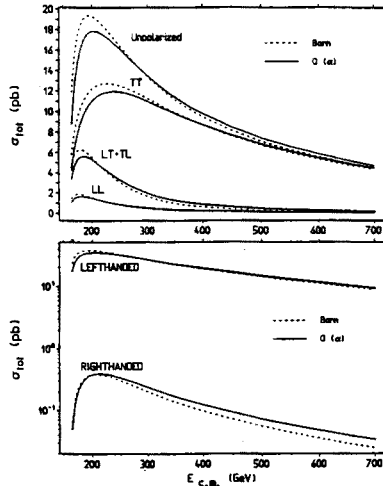


Fig. 4. Lowest order versus $O(\alpha)$ corrected cross sections including hard bremsstrahlung without kinematical cuts. Shown are the total cross section for unpolarized beams, with the individual contributions from TT, LL and LT + TL final states, and the total sections for left- and right-handed electrons.

In Fig. 4 we show the lowest order and the $O(\alpha)$ corrected cross sections including hard bremsstrahlung without any kinematical cuts. The plots show the total cross section for unpolarized beams, with the individual contributions from TT, LL and LT + TL final states, and the total sections for left- and right-handed electrons. For all the cross sections, the $O(\alpha)$ corrected results are smaller than the corresponding Born order cross sections near the peak and, at some value of the CM energy, they become slightly bigger than the lowest order results. This can be easily understood in terms of the Bonneau-Martin formula [24] which expresses the total photon corrected cross section in the leading logarithmic approximation by the radiator function times the lowest order cross section calculated at the reduced CM energy $s' = s(1 - x)$. At the threshold, where the cross section raises steeply, despite the fact that the emitted photon is rather soft, a small shift of the energy scale to lower values results in substantially smaller value of the radiatively corrected cross section. Similarly, for high CM energies, the emission of a very hard photon shifts the energy scale to lower values, where the lowest order cross section is bigger, and this time the radiatively corrected cross section becomes bigger than the Born one. The lowest figure illustrates a suppression of the right-handed initial polarization by two orders of magnitude relative to the left-handed polarization.

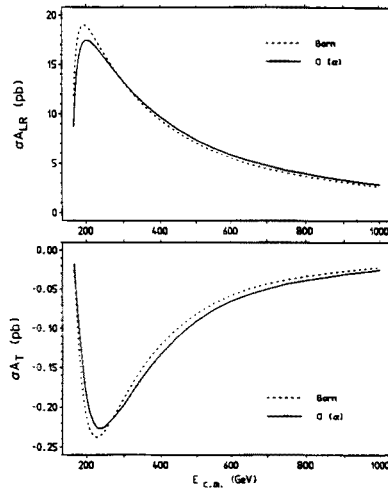


Fig. 5. Left-right asymmetry σA_{LR} and transverse asymmetry σA_T . The $O(\alpha)$ corrected asymmetries include hard bremsstrahlung without kinematical cuts.

In Fig. 5 the left-right asymmetry σA_{LR} and transverse asymmetry σA_T are shown. The $O(\alpha)$ corrected asymmetries include hard bremsstrahlung again without kinematical cuts. Since the left-right asymmetry differs from the unpolarized cross section only by the contribution of the right-handed

initial polarization (see Eqs (17) and (18)), the two quantities look very much alike. In the upper figure we assumed 100% longitudinal polarization and in the lower one, the maximal values of the transverse polarization $P_T = P'_T = 92.4\%$ [14].

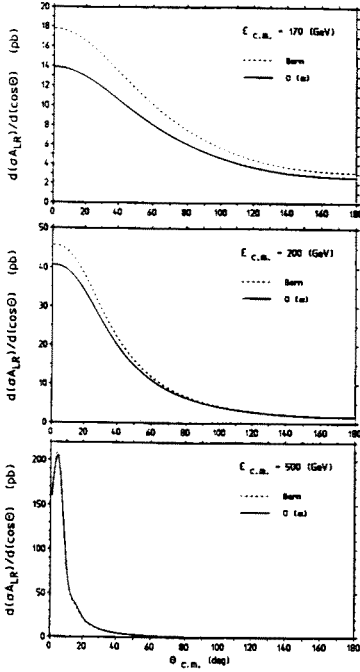


Fig.6

Fig. 6. Lowest order versus $O(\alpha)$ corrected left-right asymmetry $d(\sigma A_{LR})/d \cos \theta$ as a function of the production angle. The hard bremsstrahlung is included without kinematical cuts.

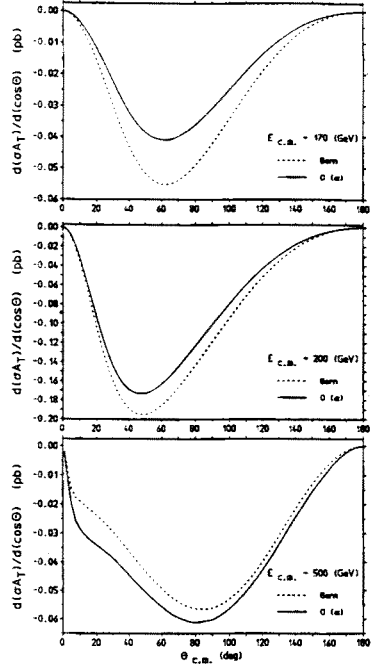


Fig.7

Fig. 7. Lowest order versus $O(\alpha)$ corrected transverse asymmetry $d(\sigma A_T)/d \cos \theta$ as a function of the production angle. The hard bremsstrahlung is included without kinematical cuts.

In Figs 6 and 7 the lowest order versus $O(\alpha)$ corrected left-right asymmetry $d(\sigma A_{LR})/d \cos \theta$ and transverse asymmetry $d(\sigma A_T)/d \cos \theta$, respectively, are shown as a function of the production angle for the CM energies of 170, 200 and 500 GeV. Again the hard bremsstrahlung is included without kinematical cuts. Finally, for comparison, in Fig. 8 we present results as in Figs 6 and 7 for the longitudinal-longitudinal (LL) final state polarization. While, for high energies, the left-right asymmetry and the LL cross section become strongly peaked in the direction of the initial electron, the transverse asymmetry assumes largest absolute values for larger angles. This can make the detection in future high energy accelerators easier.

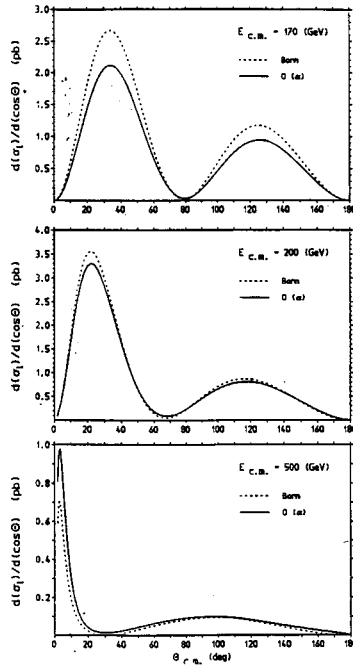


Fig. 8. Lowest order versus $O(\alpha)$ corrected longitudinal cross section $d\sigma_l/d\cos\theta$ as a function of the production angle. The hard bremsstrahlung is included without kinematical cuts.

We conclude that beam polarization provides an indispensable tool for studying the non-abelian structure of the SM of electroweak interactions. Especially the transverse beam polarization allows to study the most interesting LL polarization of the W bosons without analyzing polarizations of their decay products. Therefore, we strongly recommend to make efforts in order to measure transverse polarization at LEP 200 and in future colliders.

The author would like to thank the organizers of XVII International School of Theoretical Physics for the invitation and kind hospitality.

REFERENCES

- [1] O.P. Sushkov, V.V. Flambaum, I.B. Khriplovick, *Sov. J. Nucl. Phys.* **20**, 537 (1975); W. Alles, Ch. Boyer, A.J. Buras, *Nucl. Phys.* **B119**, 125 (1977); P. Méry, M. Perrottet, *Nucl. Phys.* **175**, 234 (1980); I.F. Ginzburg *et al.*, *Nucl. Phys.* **228**, 285 (1983).
- [2] G. Altarelli, R. Barbieri, F. Caravaglios, preprint CERN-TH 6859/93, 1993; G. Altarelli, preprint CERN-TH 6867/93, 1993; M. Bilenky, K. Kołodziej,

- M. Kuroda, D. Schildknecht, preprint BI-TP 93/46, 1993, submitted to *Phys. Lett. B*.
- [3] C.H. Lewellyn Smith, *Phys. Lett. B* **46**, 233 (1973); J.S. Bell, *Nucl. Phys. B* **60**, 427 (1973); J.M. Cornwall, D.N. Levin, G. Tiktopoulos, *Phys. Rev. Lett.* **30**, 1268 (1973); *Phys. Rev. Lett.* **31**(E), 572 (1973); *Phys. Rev.* **10**, 1145 (1974).
 - [4] Ch. Ahn, M.E. Peskin, B.W. Lynn, S. Selipsky, *Nucl. Phys.* **309**, 221 (1988).
 - [5] W. Beenakker, A. Denner, preprint CERN-TH 6928/93, 1993 and references therein.
 - [6] J.F. Guion, Z. Kunszt, *Phys. Rev. D* **33**, 665 (1986); J.C. Romão, P. Nogueira, *Z. Phys. C* **42**, 263 (1989); D. Bardin, M. Bilenky, A. Olchewsky, T. Riemann, *Phys. Lett. B* **308**, 403 (1993).
 - [7] A. Aeppli, D. Wyler, *Phys. Lett. B* **262**, 125 (1991).
 - [8] M. Lemoine, M. Veltman, *Nucl. Phys. B* **164**, 445 (1980).
 - [9] M. Böhm, A. Denner, T. Sack, W. Beenakker, F. Berends, H. Kuijf, *Nucl. Phys. B* **304**, 463 (1988).
 - [10] J. Fleischer, F. Jegerlehner, M. Zralek, *Z. Phys. C* **42**, 409 (1989).
 - [11] J.K.F. Gaemers, G.J. Gounaris, *Z. Phys. C* **1**, 259 (1979).
 - [12] K. Hagiwara, R.D. Peccei, D. Zeppenfeld, K. Hikasa, *Nucl. Phys. B* **282**, 253 (1987).
 - [13] J. Fleischer, J.L. Kneur, K. Kołodziej, M. Kuroda, D. Schildknecht, *Nucl. Phys. B* **378**, 443 (1992).
 - [14] F.M. Renard, *Basics of e^+e^- collisions*, ed. Frontières, Paris 1981.
 - [15] K. Hikasa, *Phys. Rev. D* **33**, 3203 (1986).
 - [16] J. Fleischer, K. Kołodziej, F. Jegerlehner, *Phys. Rev. D* **47**, 830 (1993).
 - [17] J. Fleischer, K. Kołodziej, F. Jegerlehner, preprint PSI-PR-93-10, 1993.
 - [18] W. Beenakker, K. Kołodziej, T. Sack, *Phys. Lett. B* **258**, 469 (1991).
 - [19] K. Kołodziej, M. Zralek, *Phys. Rev. D* **43**, 3619 (1991).
 - [20] G.P. Lepage, *J. Comp. Phys.* **27**, 192 (1978); Cornell University preprint, CLNS-80/447 (1980).
 - [21] R. Kleiss, *Z. Phys. C* **33**, 433 (1987).
 - [22] G.J. van Oldenborgh, J.A.M. Vermaseren, *Z. Phys. C* **46**, 425 (1990); G.J. van Oldenborgh, *Comput. Phys. Commun.* **66**, 1 (1991).
 - [23] C.L. Bilchak, J.D. Stroughair, *Phys. Rev. D* **30**, 1881 (1984); M. Kuroda, F.M. Renard, D. Schildknecht, *Phys. Lett. B* **183**, 366 (1986); P. Méry, M. Perrottet, F.M. Renard, *Z. Phys.* **36**, 249 (1987).
 - [24] G. Bonneau, F. Martin, *Nucl. Phys. B* **27**, 381 (1971); M. Greco, G. Pancheri, Y. Srivastava, *Nucl. Phys. B* **171**, 118 (1980); *Nucl. Phys. B* **197**, 543 (1982).